Contributions to Geophysics and Geodesy Vol. 43/1, 2013 (21–38)

On the interpolation of high-frequency gravity field signals in mountainous areas

Hussein A. ABD-ELMOTAAL[1], Norbert KÜHTREIBER[2]

[1] Civil Engineering Department, Faculty of Engineering, Minia University, Minia 61111, Egypt, e-mail: abdelmotaal@lycos.com

[2] Institute of Navigation, TU Graz, Steyrergasse 30, A-8010 Graz, Austria, e-mail: norbert.kuehtreiber@tugraz.at

Abstract: The paper presents a comparison among different techniques in interpolating high-frequency gravity field signals in mountainous areas. A gap of $1^\circ \times 1^\circ$ has been artificially created within the free-air gravity anomalies data set for Austria. The remaining data set has been used to interpolate the free-air gravity anomalies at the gap points; then a comparison between the interpolated and the data values has been carried out to determine the accuracy of the used interpolation technique. The following interpolation techniques have been used: Kriging interpolation technique from free-air gravity anomalies, traditional remove-restore technique and window technique (*Abd-Elmotaal and Kühtreiber, 2003*). For the latter two techniques, the reduced anomalies have been used to interpolate gravity anomalies at the data points of the gap using a least squares collocation technique. The effect of the topographic-isostatic masses has been restored using both techniques. A comparison between the data and interpolated values of free-air anomalies at the gap points has been carried out. The results show that the Kriging technique cannot be used for interpolating high-frequency gravity field signals in mountainous areas and the window technique gives the best results with an interpolation standard deviation of about 11 mgal. The range difference and the standard deviation of the residuals in case of the window technique are smaller than those of the traditional remove-restore technique by about 25%.

Key words: window technique, remove-restore technique, gravity interpolation, Kriging, least-squares collocation

1. Introduction

Interpolation of gravity anomalies is essential in many geodetic applications, such as geoid determination using FFT and Stokes' integral techniques. The interpolation technique introduces some errors. These errors become even

doi: 10.2478/congeo-2013-0002

higher in case of interpolating high-frequency gravity field signals in mountainous areas. One usually wants to determine the accuracy of the estimated interpolated anomalies. The current investigation considers a comparison of three interpolation techniques, namely Kriging technique using the free-air anomalies, the traditional remove-restore technique and the window technique (*Abd-Elmotaal and Kühtreiber, 2003*).

The used data sets are described (data area and gap area). The traditional remove-restore technique is described. The window technique (*Abd-Elmotaal and Kühtreiber, 2003*) within the remove-restore scheme is outlined. The harmonic analysis of the topographic-isostatic potential is then given. The reduced gravity using both traditional remove-restore and window techniques are then computed and compared. Fitting the used empirical covariance functions within the least-squares collocation technique is then given. The restore step is carried out to obtain free-air gravity anomalies at the gap data points, and the residuals (difference between data and interpolated values) at those points are computed. A wide comparison among the used interpolation techniques is carried out. The comparison is made on two different levels; the residual gravity anomalies after the remove step and the interpolation residuals.

It should be noted that many scholars have studied the gravity interpolation problem and the estimated accuracy. The reader may refer, e.g., to (*Al-Tahir, 1996; Sansò et al., 1999; Bajracharya and Sideris, 2002; Sideris, 1995; Heliani et al., 2004; Kamguia et al., 2007; Kay and Dimitrakopoulos, 2000; Völgyesi, 1993; 1995; Tóth and Völgyesi, 2002*).

2. The data

2.1. Gravity data

The gravity data set for this investigation is a set of free-air gravity anomalies at 5796 stations in Austria and neighbouring countries (Fig. 1). Figure 1 shows, more or less, a homogeneous data distribution within Austria. The gravity data covers the window ($45.7^\circ\,\mathrm{N} \le \phi \le 49.7^\circ\,\mathrm{N}$ and $8.5^\circ\,\mathrm{E} \le \lambda \le 18.2^\circ\,\mathrm{E}$).

An artificial gap of $1^\circ \times 1^\circ$ of the window $47.1^\circ\,\mathrm{N} \le \phi \le 48.1^\circ\,\mathrm{N}$ and $14.2^\circ\,\mathrm{E} \le \lambda \le 15.2^\circ\,\mathrm{E}$ has been made and all gravity data points within this

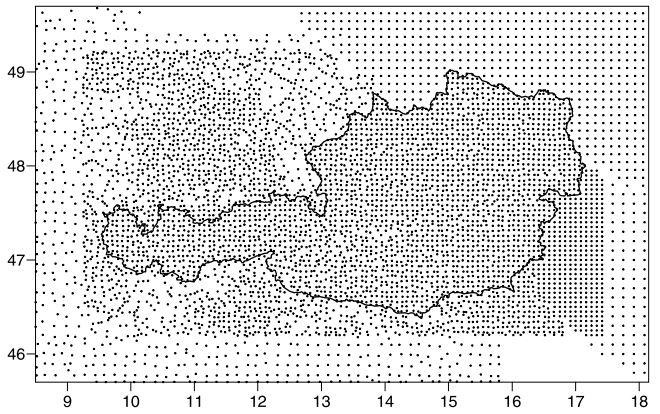

Fig. 1. Distribution of the full gravity data set.

gap (222 points) were eliminated from the full gravity data set yielding the gravity data set used for this investigation (5574 points; cf. Fig. 2).

2.2. Digital Height Models

Two different Digital Height Models (DHM) are available. A coarse model of $90'' \times 150''$ resolution in the latitude and the longitude directions, respec-

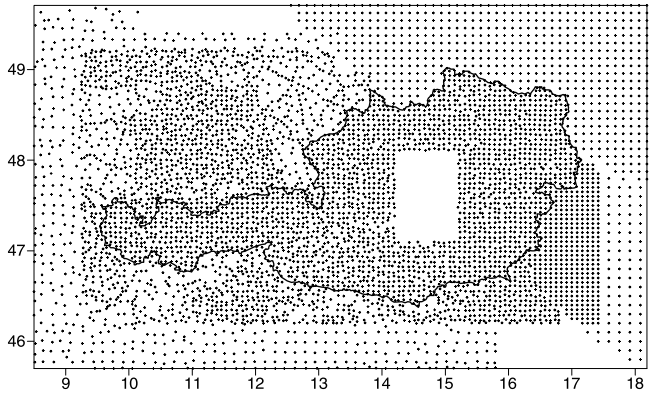

Fig. 2. Distribution of the used gravity data set after introducing the $1^\circ \times 1^\circ$ artificial gap.

tively, and a fine model of $11.25'' \times 18.75''$ resolution. The fine DHM covers the window $44.75^\circ\,\mathrm{N} \le \phi \le 50.25^\circ\,\mathrm{N}; 7.75^\circ\,\mathrm{E} \le \lambda \le 19.25^\circ\,\mathrm{E}$. The coarse DHM covers the window $40^\circ\,\mathrm{N} \le \phi \le 52^\circ\,\mathrm{N}; 5^\circ\,\mathrm{E} \le \lambda \le 22^\circ\,\mathrm{E}$.

The coarse DHM has been created by integrating the Austrian fine DHM with GTOPO30 ($30'' \times 30''$) (*Gesch and Larson, 1996*) and global bathymetry model provided by the Naval Oceanographic Office ($1' \times 1'$). Figure 3 shows the coarse digital height model used for this investigation. It shows the highly mountainous structure of the Alps.

3. Traditional remove-restore technique

Within the well-known remove-restore technique for the same gravitational quantity for the sake of smoothing the field, the effect of the topographic-isostatic masses is removed from the source gravitational data and then

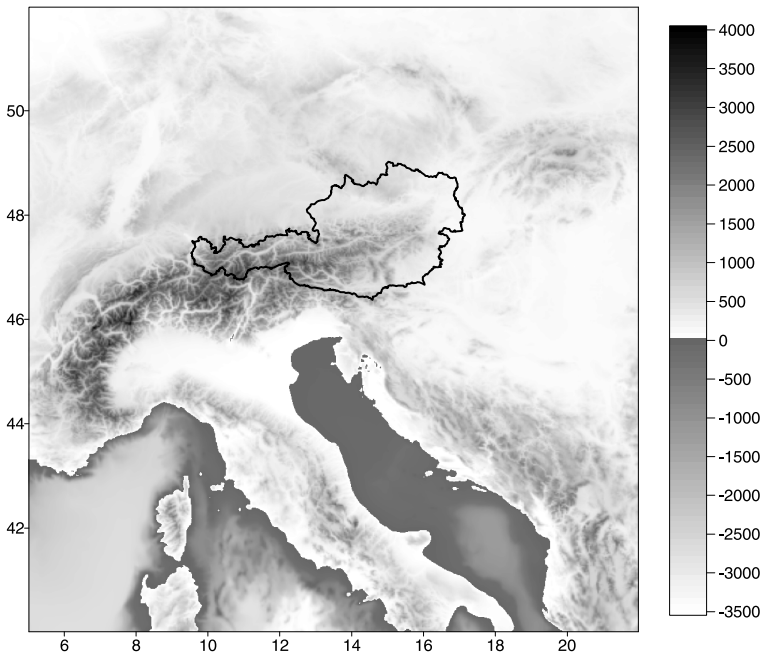

Fig. 3. The coarse ($90'' \times 150''$) digital height model. Units are in meters.

restored to the resulting interpolated values of the same gravitational quantity. For example, in the case of gravity data, the reduced gravity anomalies used in the interpolation technique in the framework of the remove-restore technique are computed by

$$\Delta g_{red} = \Delta g_F - \Delta g_{GM} - \Delta g_{TI}\,, \tag{1}$$

where Δg_F stands for the free-air anomalies, Δg_{TI} is the effect of topography and its compensation on the gravity anomalies, and Δg_{GM} is the effect of the reference field on the gravity anomalies. Thus the final restored free-air anomalies within the remove-restore technique can be expressed by:

$$\Delta g_F = \Delta g_{GM} + \Delta g_{\Delta g} + \Delta g_{TI}\,, \tag{2}$$

where $\Delta g_{\Delta g}$ stands for the interpolated gravity anomalies at the interpolated points using the reduced gravity anomalies Δg_{red} computed by (1) at the data points.

4. The window technique

The traditional way of removing the effect of the topographic-isostatic masses faces a theoretical problem. A part of the influence of the topographic-isostatic masses is removed twice as it is already included in the global reference field. This leads to some double consideration of that part of the topographic-isostatic masses. Figure 4 sketches the traditional gravity reduction for the effect of the topographic-isostatic masses. The short-wavelength part, depending on the topographic-isostatic masses, is computed for a point P for the masses inside the circle denoted by TI. Removing the effect of the long-wavelength part by a global earth's gravitational potential field normally implies removing the influence of the global topographic-isostatic masses, shown as a big rectangle in Fig. 4 denoted by EGM (here EGM stands for Global Geopotential Model). The double consideration of the topographic-isostatic masses inside the circle (double hatched) is thus seen.

A possible way to overcome this difficulty is to adapt the used reference field to the effect of the topographic-isostatic masses for a fixed data area.

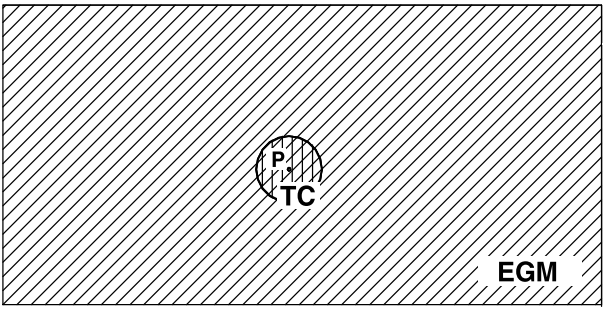

Fig. 4. The traditional remove-restore technique.

Figure 5 shows the advantage of the window remove-restore technique. Consider a measurement at point P; the short-wavelength part, depending on the topographic-isostatic masses, is now computed by using the masses of the whole data area (the small rectangle in Fig. 5). The adapted reference field is created by subtracting the effect of the topographic-isostatic masses of the data window, in terms of potential coefficients, from the reference field coefficients. Thus, removing the long-wavelength part by using this adapted reference field does not lead to a double consideration of a part of the topographic-isostatic masses (as there is no double hatched area in Fig. 5).

The remove step of the window remove-restore technique can then mathematically be written as

$$\Delta g_{red\,Win} = \Delta g_F - \Delta g_{GM\,Adapt} - \Delta g_{TI\,Win}\,, \tag{3}$$

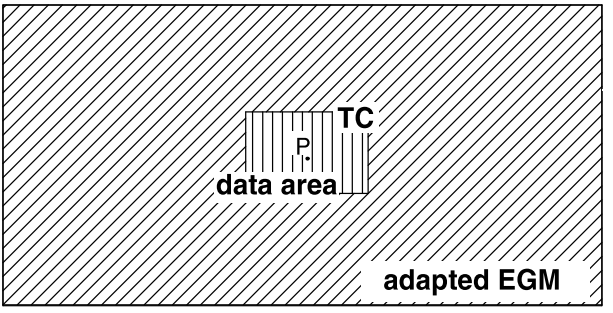

Fig. 5. The window remove-restore technique.

where $\Delta g_{GM\,Adapt}$ is the contribution of the adapted reference field and $\Delta g_{TI\,Win}$ is the effect of topography and its compensation for the fixed data window on the gravity anomalies. The restore step of the window remove-restore technique can be written as

$$\Delta g_F = \Delta g_{GM\,Adapt} + \Delta g_{\Delta g\,win} + \Delta g_{TI\,Win}\,. \tag{4}$$

Here $\Delta g_{\Delta g\,Win}$ stands for the interpolated gravity anomalies at the interpolated points using the reduced gravity anomalies $\Delta g_{red\,Win}$ computed by (3) at the data points.

5. Harmonic analysis of the topographic-isostatic potential

The harmonic coefficients of the topography and its isostatic compensation as well as the harmonic series expansion of the topographic-isostatic potential can be expressed by (*Abd-Elmotaal and Kühtreiber, 2003, pp. 78–79*):

$$T_{TI}(P) = \frac{GM}{r_P}\sum_{n=0}^{\infty}\left(\frac{R}{r_P}\right)^n \sum_{m=-n}^{n} \bar{T}_{nm}\bar{R}_{nm}(P)\,, \tag{5}$$

where $\bar{R}_{nm}(P)$ is defined by (*Hofmann-Wellenhof and Moritz, 2005, p. 21*)

$$\bar{R}_{nm}(P) = \bar{P}_{nm}(\cos\theta_P)\begin{cases}\cos\lambda_P & \text{for } n \geq 0\\ \sin\lambda_P & \text{for } n < 0\end{cases} \tag{6}$$

and GM is the geocentric gravitational constant, $\bar{P}_{nm}(\cos\theta)$ are the fully normalized Legendre functions, r_P is the radius vector and $\bar{T}_{nm}$ is given by

$$\bar{T}_{nm} = \frac{R^3}{M(2n+1)(n+3)}\iint_{\sigma}\left\{\rho_Q\left[\left(1+\frac{H_Q}{R}\right)^{n+3}-1\right]+\right.$$
$$\left.+\,\Delta\rho_Q\left(1-\frac{T_\circ}{R}\right)^{n+3}\left[\left(1-\frac{t_Q}{R-T_\circ}\right)^{n+3}-1\right]\right\}\bar{R}_{nm}(Q)\,\mathrm{d}\sigma_Q\,, \tag{7}$$

where $T_\circ$ is the normal crustal thickness, H is the topographic height, t is the compensating root/antiroot and M denotes the mass of the earth, given by

$$M \doteq \frac{4\pi R^3}{3}\,\rho_{_M}\,, \tag{8}$$

where $\rho_{_M}$ denotes the mean earth's density and ρ is given by

$$\begin{aligned} \rho &= \rho_\circ && \text{for } H \geq 0\,, \\ \rho &= \rho_\circ - \rho_w && \text{for } H < 0\,, \end{aligned} \tag{9}$$

where $\rho_\circ$ denotes the density of the topography and ρ_w is the density of ocean's water. The density contrast $\Delta\rho$ is given by

$$\Delta\rho = \rho_1 - \rho_\circ\,, \tag{10}$$

where ρ_1 is the density of the upper mantle.

For the practical determination of the harmonic coefficients of the topographic-isostatic potential, (7) may be written as

$$\begin{aligned} \bar{T}_{nm} = \frac{3\Delta\phi\,\Delta\lambda}{4\pi\rho_{_M}(2n+1)(n+3)} \sum_i^{\phi}\sum_j^{\lambda} \Bigg\{ \rho_{ij} \left[\left(1+\frac{H_{ij}}{R}\right)^{n+3} - 1 \right] + \\ + \Delta\rho_{ij} \left(1-\frac{T_\circ}{R}\right)^{n+3} \left[\left(1-\frac{t_{ij}}{R-T_\circ}\right)^{n+3} - 1 \right] \Bigg\} \times \\ \times \left\{ \begin{matrix} \cos m\lambda_j \\ \sin m\lambda_j \end{matrix} \right\} \bar{P}_{nm}(\cos\theta_i)\cos\phi_i\,, \end{aligned} \tag{11}$$

where $\sum$ denotes the summation along ϕ and λ, $\Delta\phi$ and $\Delta\lambda$ are the grid sizes of the used Digital Height Model in the latitude and the longitude directions, respectively.

6. Gravity reduction

The following parameter set has been used during the gravity reduction as they empirically proved to fit the Austrian gravity field to a good extent (cf. *Kühtreiber and Abd-Elmotaal, 2001*):

$$T_\circ = 30 \text{ km}\,, \tag{12}$$

$$\rho_\circ = 2.67 \text{ g/cm}^3\,, \tag{13}$$

$$\Delta\rho = 0.20 \text{ g/cm}^3\,. \tag{14}$$

The EGM96 geopotential model has been used for the traditional remove-restore technique. An adapted reference field has been created by subtracting the potential coefficients of the topographic-isostatic masses of the data window ($40^\circ\,\mathrm{N} \leq \phi \leq 52^\circ\,\mathrm{N}; 5^\circ\,\mathrm{E} \leq \lambda \leq 22^\circ\,\mathrm{E}$) computed by (11) from the EGM96 coefficients. This adapted reference field has been used for the window remove-restore technique.

Table 1 shows the statistics of the data free-air anomalies as well as the reduced anomalies for both the traditional and the window remove-restore techniques. It shows that using the window technique gives the best reduced gravity anomalies compared to the traditional remove-restore technique. The range has dropped by its one-fourth and the standard deviation drops by about 10%. Also the reduced anomalies are perfectly centered (un-biased). This property makes the window-technique reduced anomalies best suited for interpolation and other geodetic purposes.

Table 1. Statistics of the reduced gravity anomalies

reduced gravity	statistical parameters			
	min.	max.	average	st. dev.
	mgal	mgal	mgal	mgal
Δg_F	−154.11	187.21	9.76	42.24
$\Delta g_F - \Delta g_{GM} - \Delta g_{TI}$	−123.46	82.16	−19.53	25.91
$\Delta g_F - \Delta g_{GM\ Adapt} - \Delta g_{TI\ Win}$	−71.97	85.41	0.10	23.53

7. Least-squares collocation technique

The interpolated gravity anomalies at the interpolation points $\Delta g_{\Delta g}$ using the reduced gravity anomalies at the data points is computed in this investigation using the least-squares collocation technique. The normalized observation equation for the least-squares collocation technique can be written as (*Moritz, 1980, p. 99*)

$$l = t + n\,, \tag{15}$$

where l denotes the measurements, n denotes the measuring errors (noise) and t denotes the signal part of the measurements, which is related to the earth's gravitational field. Equation (15) refers to the so-called *least-squares*

collocation without parameters.

The estimated signals $\hat{s}$ are given by (*ibid., p. 102*)

$$\hat{s} = C_{st} \left(C_{tt} + C_{nn}\right)^{-1} l \,, \tag{16}$$

where C_{st} is the cross-covariance matrix between the measurements and the estimated signals, C_{tt} is the auto-covariance matrix of the measurements and C_{nn} is the covariance matrix of the noise. The error covariance matrix of the estimated signals E_{ss} is given by (*ibid., p. 105*)

$$E_{ss} = C_{ss} - C_{st} \left(C_{tt} + C_{nn}\right)^{-1} C_{st}^T \tag{17}$$

where C_{ss} is the auto-covariance matrix of the estimated signals.

It should be noted that the quantities t and s are related to the earth's gravitational field, which are linear functionals of the anomalous potential T. Hence the matrices C_{tt}, C_{st} and C_{ss} can be obtained from the basic covariance function of the anomalous potential by covariance propagation (*ibid., pp. 86–87*). For practical applications, the covariance function of the gravity anomalies plays the role of the basic covariance function, from which all other covariance matrices can be derived.

8. Covariance functions

The used covariance function model in this investigation is the well known Tscherning-Rapp covariance function model. The global covariance function of the gravity anomalies $C_g(P,Q)$ is given by (*Tscherning and Rapp, 1974, p. 29*)

$$C_g(P,Q) = A \sum_{n=3}^{\infty} \frac{n-1}{(n-2)(n+B)} \, s^{n+2} P_n(\cos\psi) \,, \tag{18}$$

where $P_n(\cos\psi)$ denotes the Legendre polynomial of degree n, ψ is the spherical distance between P and Q and A, B and s are the model parameters. Closed expression for (18) is available in (*ibid., p. 45*).

The Tscherning-Rapp local covariance function of gravity anomalies $C(P,Q)$ can be defined as

$$C(P,Q) = A \sum_{NN+1}^{\infty} \frac{n-1}{(n-2)(n+B)} \, s^{n+2} P_n(\cos\psi) \,. \tag{19}$$

This expression may be written in the form (*ibid., p. 62*)

$$C(P,Q) = A\sum_{n=3}^{\infty}\frac{n-1}{(n-2)(n+B)}\,s^{n+2}P_n(\cos\psi) - \\ -A\sum_{3}^{NN}\frac{n-1}{(n-2)(n+B)}\,s^{n+2}P_n(\cos\psi) = \\ = C_g(P,Q) - A\sum_{n=3}^{NN}\frac{n-1}{(n-2)(n+B)}\,s^{n+2}P_n(\cos\psi)\,, \tag{20}$$

where $C_g(P,Q)$ is given by (18) and its closed form.

Modelling the covariance function means in practice fitting the empirically determined covariance function (through its three essential parameters; the variance $C_\circ$, the correlation length ξ and the variance of the horizontal gradient $G_{\circ H}$) to the covariance function model. Hence the four parameters A, B, NN and s are to be determined through this fitting procedure.

A program has been written to fit the empirically determined variance $C_\circ$ and correlation length ξ of the gravity anomalies covariance function to the Tscherning-Rapp covariance function model in such a way that it determines the best horizontal gradient $G_{\circ H}$ that it gives the minimum σ_V^2, defined by

$$\sigma_V^2 = \frac{1}{n}\sum_{i=1}^{n} V_i^2, \tag{21}$$

where V stands for the covariance residual (empirically determined minus modelled) at the empirical covariance function points n. This assures best fitting to the empirically determined covariance function.

Table 2 shows the essential parameters of the empirical covariance function of the gravity anomalies for both cases (i.e., using traditional remove-restore technique and using window technique). The values of the horizontal

Table 2. Essential parameters of the empirical gravity anomaly covariance functions

reduction technique	$C_\circ$	ξ	$G_{\circ H}$
	mgal^2	km	E^2
Traditional remove-restore	671.08	59.84	52
window	553.59	46.33	52

gradient variance $G_{\circ H}$ have been estimated with the procedure described above.

Table 3 shows the Tscherning-Rapp covariance function model parameters for both cases using traditional remove-restore technique and using window technique. A fixed value of

$$B = 24 \text{ exact}$$

has been chosen for all cases. This value matches the same value for the global gravity anomaly covariance function.

Table 3. Tscherning-Rapp covariance function model parameters

reduction technique	s	A	NN
	—	mgal^2	—
Traditional remove-restore	0.998150	626.32	50
Window	0.997950	802.87	86

Figure 6 shows the empirical and modelled covariance functions in case of using traditional remove-restore technique. It shows a very good fitting of the empirical covariance function. This illustrates that the used fitting technique of the empirical covariance function works best.

Figure 7 shows the empirical and modelled covariance functions in case of using window technique. It also shows a very good fitting of the empirical covariance function.

9. Estimated free-air gravity anomalies

As stated before, all three interpolation techniques (namely, Kriging interpolation technique from free-air gravity anomalies, least-squares collocation using both traditional remove-restore technique and window technique) have been used to estimate the free-air gravity anomalies at the gap points. The interpolated values are then compared to the data values at the gap points to estimate the accuracy of the interpolation technique.

Table 4 shows the statistics of the residuals of the estimated free-air anomalies at the gap points. It shows that the Kriging technique cannot

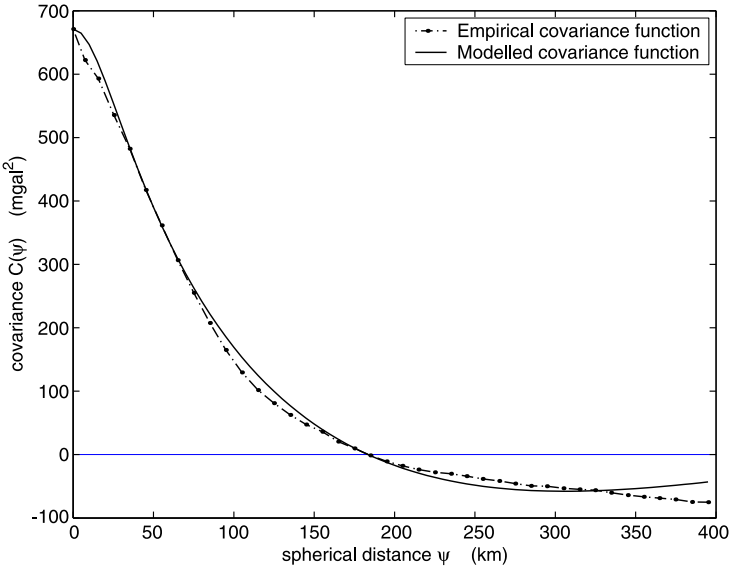

Fig. 6. Empirical and modelled covariance functions in case of using traditional remove-restore technique.

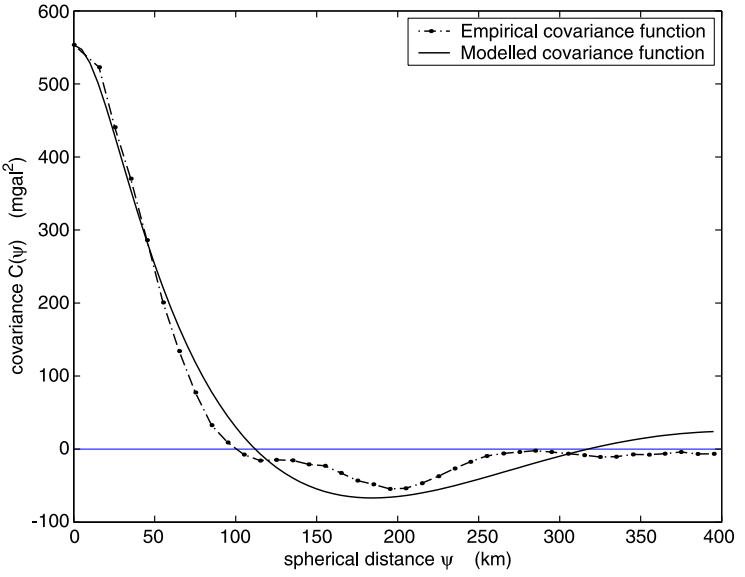

Fig. 7. Empirical and modelled covariance functions in case of using window technique.

Table 4. Statistics of the residuals of the estimated free-air anomalies at the gap points

interpolation technique	statistical parameters			
	min.	max.	average	st. dev.
	mgal	mgal	mgal	mgal
Kriging (free-air)	−129.77	72.60	−40.45	43.74
Collocation (remove-restore)	−52.44	2.82	−19.08	15.03
Collocation (window)	−38.75	4.72	−11.55	11.42

be used for interpolating free-air gravity anomalies in mountainous areas as it gives very high values of residuals in terms of both the range and the standard deviation. Table 4 shows also that the collocation interpolation

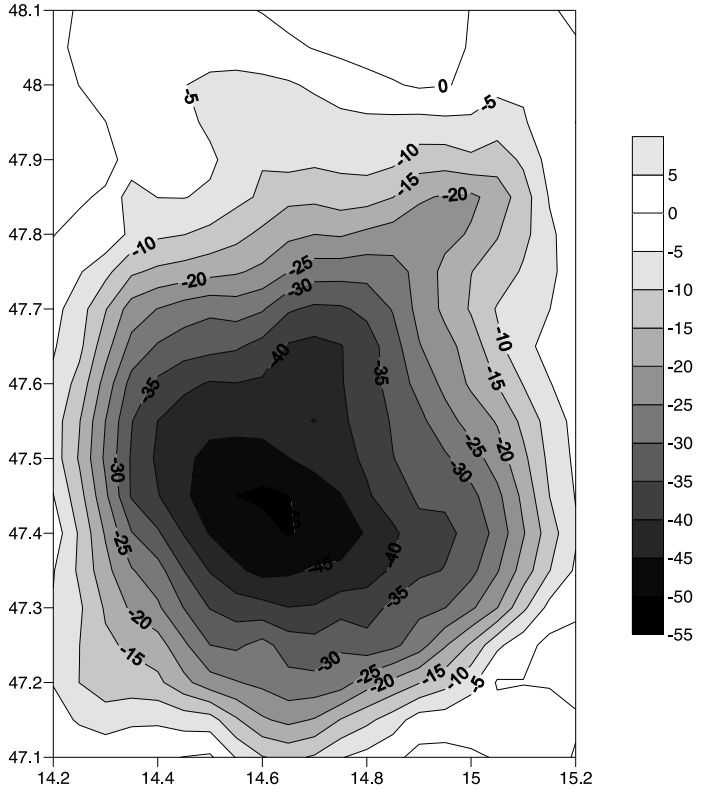

Fig. 8. Residuals of the estimated free-air anomalies at the gap points using collocation interpolation with traditional remove-restore reduction technique. Units are in mgals.

with window reduction technique gives the best results. Both the range difference and the standard deviation of the residuals in case of collocation interpolation with window technique are smaller than those of collocation interpolation with traditional remove-restore technique by about 25%. Moreover, the residuals are more centered (less biased) in case of collocation with window technique.

Figure 8 shows the residuals of the estimated free-air anomalies at the gap points using collocation interpolation with traditional remove-restore reduction technique.

Figure 9 shows the residuals of the estimated free-air anomalies at the gap points using collocation interpolation with window reduction technique.

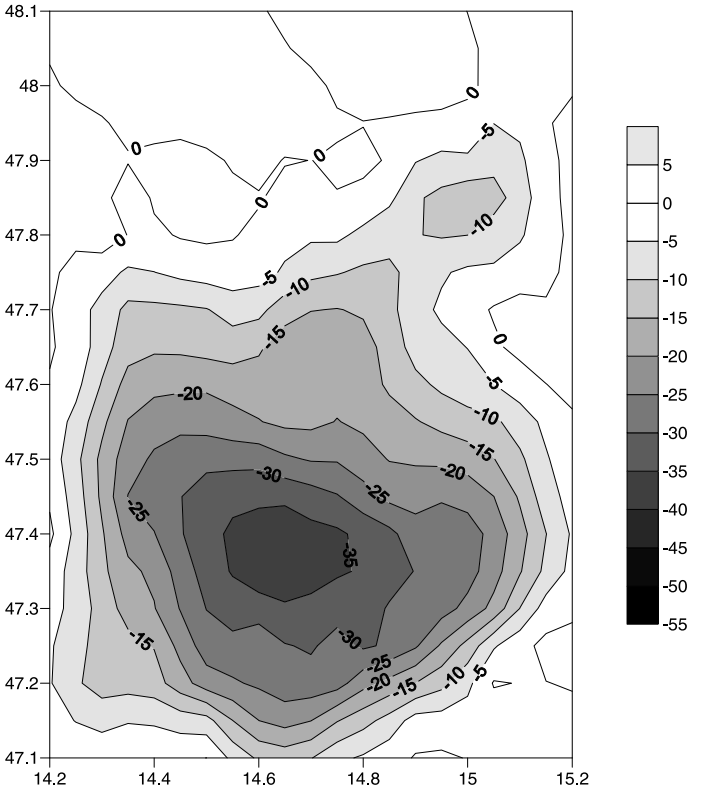

Fig. 9. Residuals of the estimated free-air anomalies at the gap points using collocation interpolation with window reduction technique. Unites are in mgals.

Comparing Fig. 8 with Fig. 9 shows that window reduction technique gives significantly less residuals.

Figure 10 shows the DHM for the gap area. Comparing Figs. 8, 9 and 10 shows that the remaining residuals of the estimated free-air anomalies at the gap points using collocation interpolation are correlated with topography.

10. Conclusion

The paper shows a comparison between the traditional remove-restore technique and the window technique in interpolating high-frequency gravity

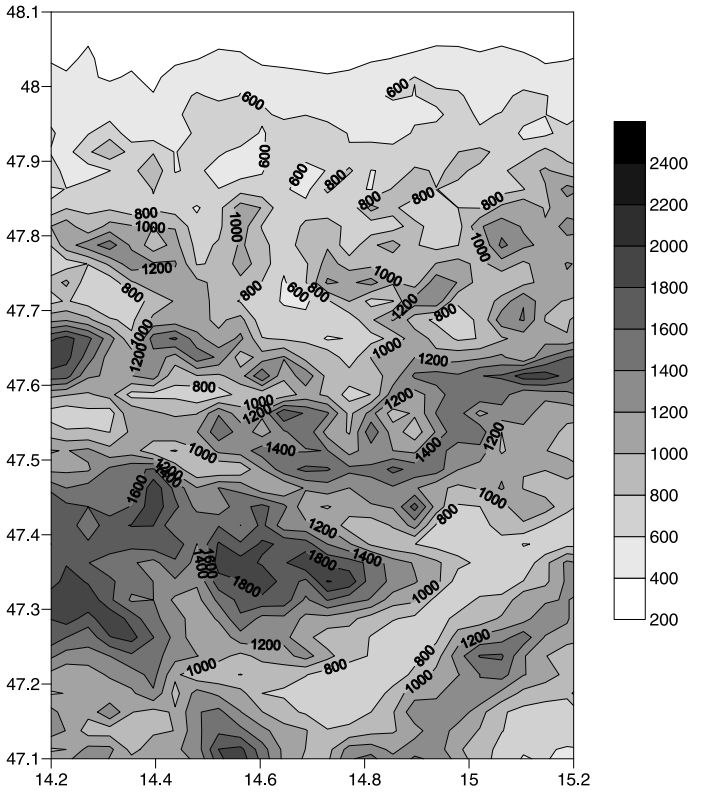

Fig. 10. Digital Hight Model for the gap area. Units are in meters.

field signals in mountainous areas. The reduced anomalies using the window technique are unbiased and have a smaller standard deviation than those using the traditional remove-restore technique. The empirical covariance function of the reduced anomalies using the window technique goes practically to zero at about 250 km.

The paper introduces an efficient covariance function fitting technique. This technique gives a good fitting of the used covariance functions within the current investigation.

The results show that the window technique gives better interpolation accuracy (less residuals between the observed and interpolated gravity anomalies) with a standard deviation of about 11 mgal. The range difference and the standard deviation of the residuals in case of the window technique are smaller than those of the traditional remove-restore technique by about 25%.

Finally, it should be noted that the interpolation accuracy has a stronger relation with topography in case of using the traditional remove-restore technique.

References

Abd-Elmotaal H., Kühtreiber N., 2003: Geoid Determination Using Adapted Reference Field, Seismic Moho Depths and Variable Density Contrast. Journal of Geodesy, **77**, 77–85.

Al-Tahir R., 1996: Interpolation and Analysis in Hierarchical Surface Reconstruction. Department of Geodetic Science, The Ohio State University, Columbus, Ohio, **435**.

Bajracharya S., Sideris M. G., 2002: The Effect of Different Terrain Reductions on Gravity Interpolation and on Helmert Geoid Determination. Presented at EGS XXVII General Assembly, Nice, 21-26 April 2002.

Gesch D. B., Larson K. S., 1996: Techniques for Development of Global 1-Kilometer Digital Elevation Models. In: Pecora Thirteen, Human Interactions with the Environment - Perspectives from Space, Sioux Falls, South Dakota, August 20–22, 1996.

Heliani L. S., Fukuda Y., Takemoto S., 2004: Simulation of the Indonesian land gravity data using a digital terrain model data. Earth Planets Space, **56**, 15–24.

Hofmann-Wellenhof B., Moritz H., 2005: Physical Geodesy. Springer, Wien.

Kamguia1 J., Tabod C. T., Tadjou J. M., Manguelle-Dicoum E., Nouayou R., Kande L. H., 2007: Accurate Gravity Anomaly Interpolation: A Case-Study in Cameroon, Central Africa. Earth Sci. Res. J., **11**, (2, December, 2007), 108–117.

Kay M., Dimitrakopoulos R., 2000: Integrated Interpolation Methods for Geophysical Data: Applications to Mineral Exploration. Natural Resources Research, **9**, 1, 53–64.

Kühtreiber N., Abd-Elmotaal H., 2001: Gravimetric Geoid Computation for Austria Using Seismic Moho Data. In: Sideris M., edt. (2001) Gravity, Geoid and Geodynamics 2000, International Association of Geodesy Symposia, Banff, Canada, July 31 – August 4, 2000, **123**, 311–316.

Moritz H., 1980: Advanced Physical Geodesy. Herbert Wichmann, Karlsruhe (2nd ed., 1989).

Sansò F., Venuti G., Tscherning C. C., 1999: A theorem of insensitivity of the collocation solution to variations of the metric of the interpolation space. In: International Association of Geodesy Symposia, "Geodesy beyond 2000. The challenges of the first decade", K. P. Schwarz ed., Springer-Verlag, Berlin, **121**, 233–240.

Sideris M. G., 1995: Fourier Geoid Determination with Irregular Data. Journal of Geodesy, **70**, 2–12.

Tóth Gy., Völgyesi L., 2002: Comparison of Interpolation and Collocation Techniques Using Torsion Balance Data. Reports on Geodesy, Warsaw University of Technology, **61**, 1, 171–182.

Tscherning C. C., Rapp R. H., 1974: Closed covariance expression for gravity anomalies, geoid undulations and deflections of the vertical by anomaly degree variance models. Department of Geodetic Science, The Ohio State University, Columbus, Ohio, **208**.

Völgyesi L., 1993: Interpolation of Deflection of the Vertical Based on Gravity Gradients. Periodica Polytechnica Civ. Eng., **37**, 2, 137–166.

Völgyesi L., 1995: Test Interpolation of Deflection of the Vertical in Hungary Based on Gravity Gradients. Periodica Polytechnica Civ. Eng., **39**, 1, 37–75.